Enhanced Magnon-Photon Coupling at the Angular Momentum Compensation Point of Ferrimagnets

Jaechul Shim,[1,2] Seok-Jong Kim,[3] Se Kwon Kim,[4,5,*] and Kyung-Jin Lee[1,3,†]
[1]Department of Materials Science and Engineering, Korea University, Seoul 02841, Korea
[2]Semiconductor R&D Center, Samsung Electronics Co. Ltd., Hwaseong, Gyeonggi 18448, Korea
[3]KU-KIST Graduate School of Converging Science and Technology, Korea University, Seoul 02841, Korea
[4]Department of Physics, KAIST, Daejeon 34141, Korea
[5]Department of Physics and Astronomy, University of Missouri, Columbia, Missouri 65211, USA

(Received 6 March 2020; accepted 18 June 2020; published 10 July 2020)

We theoretically show that the coupling between magnons in an antiferromagnetically coupled ferrimagnet and microwave photons in a cavity is largely enhanced at the angular momentum compensation point (T_A) when T_A is distinct from the magnetization compensation point. The origin of the enhanced magnon-photon coupling at T_A is identified as the antiferromagnetic spin dynamics combined with a finite magnetization. Moreover, we show that strong magnon-photon coupling can be achieved at high excitation frequency in a ferrimagnet, which is challenging to achieve for a ferromagnet due to low magnon frequency and for an antiferromagnet due to weak magnon-photon coupling. Our results will invigorate research on magnon-photon coupling by proposing ferrimagnets as a versatile platform that offers advantages of both ferromagnets and antiferromagnets.

DOI: 10.1103/PhysRevLett.125.027205

Introduction.—Quantum information technology [1] involves process, storage, transmission, and transduction of quantum information. Several physical systems have been examined to fulfill the functional tasks [2–5]. By selectively combining proper physical platforms, various hybrid quantum systems have also been designed to build a multifunctional quantum information processing system [6,7]. Photons in a microwave cavity mediate qubits from one physical constituent to another [6]. For storage and transduction of qubits, the spin ensemble [8,9] is an adequate candidate because spins allow longer coherence time than other physical quantities due to limited dissipative channel to environment.

A strong coupling of the spin ensemble to other components in hybrid quantum system is essential for suppressing the loss of quantum information during the process. As the coupling strength is enhanced by a factor of $\sqrt{N}$, where N is the spin density [10], a strong magnon-photon coupling in magnetic materials was theoretically predicted [11] and experimentally confirmed [12], leading to recent intensive studies on magnon-photon coupling in magnetic materials with various aspects [13–34], including single magnon detection [18], magnon dressed state [23], spin-information transfer between two magnets through cavity photons [17,24], and attractive level crossing [26–28,31].

For widespread application, not only strong magnon-photon coupling but also high excitation frequency (i.e., high magnon frequency) is required. In particular, the latter allows us to expand the frequency window where the transduction of quantum information occurs. Most studies so far have focused on the coupling between ferromagnetic magnons and microwave photons. We note that although yttrium iron garnet (YIG), a ferrimagnetic insulator with antiferromagnetically coupled Fe moments, has been widely used for the magnon-photon coupling, its magnon dynamics is well described by ferromagnetic magnon theories [12–31] because it is far from the compensation condition. In this respect, YIG can be considered as a ferromagnet (FM) with a reduced moment. For ferromagnets, the magnon-photon coupling strength is limited below a few hundred megahertz at the magnon frequency in gigahertz ranges [12–31]. On the other hand, recent studies found that antiferromagnetic magnons also couple to microwave photons [32–34]. For antiferromagnets (AFMs), the magnon frequency is much higher than for ferromagnets because of the manifestation of antiferromagnetic exchange interaction [35–37]. The magnon-photon coupling is, however, much weaker for antiferromagnets than for ferromagnets [34] because of net zero magnetic moment in equilibrium. Therefore, it has remained challenging to achieve both high excitation frequency and strong magnon-photon coupling in ferromagnets or antiferromagnets.

In this Letter, we theoretically show that this challenge can be overcome by employing a class of ferrimagnets (FIMs). The necessary condition is that two inequivalent spin moments with different Landé-g factors are coupled antiferromagnetically, which is satisfied in some rare-earth (RE) transition-metal (TM) ferrimagnets. This condition allows for a finite net magnetic moment, thus a finite Zeeman coupling, at the angular momentum compensation point T_A where the net spin density vanishes. The nature of

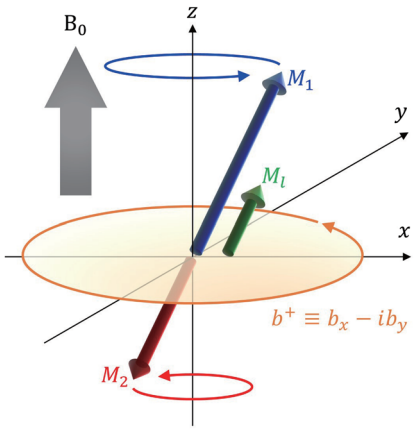

FIG. 1. An antiferromagnetically coupled ferrimagnet consisting of $\mathbf{M}_1$ and $\mathbf{M}_2$ is coupled to a circularly polarized microwave field b^+. $M_l(=|\mathbf{M}_1|-|\mathbf{M}_2|)$ is the net magnetic moment and B_0 is the external magnetic field along the uniaxial easy axis (z direction).

spin dynamics in ferrimagnets becomes antiferromagnetic at T_A since the vanishing net spin density inhibits spin-rotational motion as in antiferromagnets [38–44]. Around T_A, the magnon-photon coupling is enhanced by virtue of the exchange enhancement [45,46]. Moreover, a finite Zeeman coupling at T_A further enhances the magnon-photon coupling. Therefore, the exchange enhancement combined with a finite Zeeman coupling at T_A allows for a strong magnon-photon coupling at high magnon frequency. We envision that ferrimagnets would accelerate the advancement of cavity spintronics by offering unique features that are not readily accessible with more conventional ferromagnets and antiferromagnets.

Theoretical model.—Both quantum mechanical [11,30] and semiclassical [17] approaches are able to describe the magnon-photon coupling. We use the latter in this work. We consider a bipartite ferrimagnet with uniaxial anisotropy, which consists of two sublattices labeled by an index i (Fig. 1). The spin density vector at the ith sublattice is $s_i\mathbf{n}_i(=M_i\hbar\mathbf{n}_i/g_i\mu_B)$, with the spin density s_i, the unit vector $\mathbf{n}_i$, the magnetization M_i, the reduced Planck constant $\hbar$, the Landé-g factor g_i, and the Bohr magneton μ_B. Introducing the staggered vector $[\mathbf{n}=(\mathbf{n}_1-\mathbf{n}_2)/2]$ (serving as an order parameter) and the small magnetization vector $[\mathbf{m}=(\mathbf{n}_1+\mathbf{n}_2)]$, the Lagrangian density for the ferrimagnet is given by [39,43,47]

$$\mathcal{L}=\left[-\frac{s}{2}\dot{\mathbf{n}}\cdot(\mathbf{n}\times\mathbf{m})-\delta_s\mathbf{a}(\mathbf{n})\cdot\dot{\mathbf{n}}\right]-\mathcal{U}, \tag{1}$$

where $s(=s_1+s_2)$ is the sum of spin densities, $\delta_s(=s_1-s_2)$ is the net spin density, and $\mathbf{a}(\mathbf{n})$ is the vector potential for magnetic monopole. The potential-energy density $\mathcal{U}$ includes the exchange, anisotropy, and Zeeman energies as

$$\mathcal{U}=\frac{a|\mathbf{m}|^2}{2}+\frac{A(\nabla\mathbf{n})^2}{2}-\frac{K_u n_z^2}{2}-\mathbf{B}\cdot\left(M_l\mathbf{n}+M_t\frac{\mathbf{m}}{2}\right), \tag{2}$$

where a (A) is the homogeneous (inhomogeneous) exchange, K_u is the easy-axis anisotropy along the z axis, and $M_l(=M_1-M_2)$ and $M_t(=M_1+M_2)$ represent the magnetizations longitudinal and transverse to $\mathbf{n}$, respectively. The magnetic field $\mathbf{B}$ is $\mathbf{B}=(b_x,b_y,B_0)$, where $b_{x(y)}$ is the magnetic field part of microwaves and B_0 is the external field. In this work, we consider magnon excitations on top of a uniformly magnetized sample and disregard dissipation-related terms assuming a low damping.

By finding the stationary solution for the above Lagrangian, $\mathbf{m}$ can be expressed in terms of $\mathbf{n}$ and $\mathbf{B}$ as

$$\mathbf{m}=\frac{2\rho}{s}\mathbf{n}\times\dot{\mathbf{n}}+\frac{2\rho g_t}{s}\mathbf{B}-\frac{2\rho g_t}{s}(\mathbf{n}\cdot\mathbf{B})\mathbf{n}, \tag{3}$$

where $\rho=s^2/4a$ represents the inertia and $g_t=M_t/s$ is the transverse g factor (with respect to $\mathbf{n}$). By integrating out $\mathbf{m}$, we obtain the equation of motion for $\mathbf{n}$:

$$\delta_s\dot{\mathbf{n}}+\rho\mathbf{n}\times\ddot{\mathbf{n}}-\rho g_t[2(\mathbf{n}\cdot\mathbf{B})\dot{\mathbf{n}}+(\mathbf{n}\cdot\dot{\mathbf{B}})\mathbf{n}-\dot{\mathbf{B}}]=\mathbf{n}\times\mathbf{f}_\mathbf{n}, \tag{4}$$

where $\mathbf{f}_\mathbf{n}=M_l\mathbf{B}-\rho g_t^2(\mathbf{n}\cdot\mathbf{B})\mathbf{B}+K_u n_z\hat{\mathbf{z}}$ is the effective field conjugate to $\mathbf{n}$. At T_A, where $\delta_s=0$, the obtained equation of motion for the dynamics of ferrimagnets is reduced to that for the dynamics of antiferromagnets [48].

On the other hand, the equation of motion for microwave dynamics in a cavity is given by [17]

$$\dot{b}_{x(y)}+\omega_c^2\int b_{x(y)}dt+K^2\mu_0\dot{M}_{x(y)}=0, \tag{5}$$

where ω_c is the microwave frequency, K is the dimensionless magnon-photon coupling parameter through the Faraday induction and Ampère's law, μ_0 is the permeability in vacuum, and $M_{x(y)}$ is the $x(y)$ component of the sum of sublattice magnetizations: $M_{x(y)}=(M_l\mathbf{n}+M_t\mathbf{m}/2)_{x(y)}$.

Assuming harmonic time dependence of $n^+(\equiv n_x-in_y=ne^{-i\omega t})$ and $b^+(\equiv b_x-ib_y=be^{-i\omega t})$, and implementing the rotating-wave approximation, we linearize the above two equations of motion and obtain

$$M\begin{pmatrix}n^+\\b^+\end{pmatrix}=0, \tag{6}$$

where M is a 2×2 matrix given by

$$M=\begin{pmatrix}\rho(\omega-\omega_+)(\omega-\omega_-) & \rho g_t(\omega-\omega_{nh})\\ \rho g_t\mu_0K^2\omega^2(\omega-\omega_{nh}) & (1+\rho g_t^2\mu_0K^2)\omega^2-\omega_c^2\end{pmatrix}, \tag{7}$$

the magnon frequencies $\omega_\pm$ are given by

$$\omega_\pm = \frac{\pm\sqrt{\delta_s^2 - 4\rho\delta_s g_t B_0 + 4\rho(K_u + M_l B_0)} - \delta_s}{2\rho} + g_t B_0, \quad (8)$$

and $\omega_{nh} = g_t B_0 - M_l/\rho g_t$.

Ferrimagnets have both right-handed and left-handed modes [i.e., $\pm$ sign in Eq. (8)]. We focus on one of the two modes, namely ω_+, since two magnon modes do not mix in the system with spin-rotational symmetry as in this work, and microwave photons with a definite handedness couple to only one mode with the same handedness. It is straightforward to convert all results obtained below for the other mode, namely ω_-. Solving Eq. (6) for eigenfrequencies ω of the coupled system gives the magnon-photon coupling strength Ω, which is defined as a gap between two positive eigenfrequencies at $\omega_c = \omega_+$.

Magnon-photon coupling at T_A.—Given that K is on the order of 0.01 [17], we obtain the magnon-photon coupling Ω by approximating the matrix M of Eq. (6) in the vicinity of the magnon frequency, $|\omega - \omega_+| \ll \omega_+$, i.e., by extracting the leading-order contributions of each matrix element with respect to $(\omega - \omega_+)$ and K:

$$M \approx \begin{pmatrix} \rho\Delta_m(\omega - \omega_+) & \rho g_t(\omega_+ - \omega_{nh}) \\ \rho g_t \mu_0 K^2 \omega_+^2(\omega_+ - \omega_{nh}) & 2\omega_+(\omega - \omega_+) \end{pmatrix}, \quad (9)$$

where $\Delta_m = (\omega_+ - \omega_-)$. From $\det(M) = 0$, we obtain two eigenfrequencies:

$$\omega = \omega_+ \pm K|\omega_+ - \omega_{nh}|\sqrt{\frac{\mu_0\rho g_t^2\omega_+}{2\Delta_m}}. \quad (10)$$

The corresponding gap at the mode-crossing point is

$$\Omega = K|\omega_+ - \omega_{nh}|\sqrt{\frac{2\mu_0\rho g_t^2\omega_+}{\Delta_m}}. \quad (11)$$

For a legitimate comparison of the magnon-photon coupling efficiency across various ferrimagnets with distinct material parameters, we define a dimensionless effective magnon-photon coupling strength ζ as

$$\zeta = \frac{\Omega}{\sqrt{\omega_+\omega_{T_A}}} = K|\omega_+ - \omega_{nh}|\sqrt{\frac{2\mu_0\rho g_t^2}{\Delta_m\omega_{T_A}}}, \quad (12)$$

where $\omega_{T_A}(=\sqrt{K_u/\rho})$ is ω_+ at T_A. Here, the factor $1/\sqrt{\omega_+}$ is introduced since Ω is known to be proportional to $\sqrt{\omega_c}$ $(=\sqrt{\omega_+}$ in our case) regardless of the sign of microscopic exchange interaction [34], whereas the factor $1/\sqrt{\omega_{T_A}}$ is introduced to make ζ dimensionless.

To get an insight into the effective coupling strength ζ in the vicinity of T_A, we set $B_0 = 0$ and $\delta_s = 0$ for $|\omega_+ - \omega_{nh}|$ of Eq. (12) and then obtain

$$\zeta = K\left(\sqrt{\mu_0\rho g_t^2 K_u} + \sqrt{\mu_0 M_l^2}\right)\sqrt{\frac{2}{\rho\Delta_m\omega_{T_A}}}. \quad (13)$$

Let us consider the factor embraced by parentheses. We note that $\sqrt{\mu_0\rho g_t^2} = \sqrt{\mu_0 M_t^2/(4a)}$. When replacing $M_t = M_1 + M_2$ by $2M_1$ (assuming $M_1 \approx M_2$) and a by J/d^3 with J the microscopic Heisenberg exchange energy and d the lattice constant, we obtain $\sqrt{\mu_0 M_t^2/(4a)} \sim \sqrt{\mu_0 M_1^2 d^3/J}$. This is the square root of the ratio of the magnetostatic energy to the exchange energy, which is much smaller than 1. In the vicinity of T_A, therefore, $\sqrt{\mu_0 M_l^2}$ should dominate $\sqrt{\mu_0\rho g_t^2 K_u}$ unless K_u is very large. Ignoring $\sqrt{\mu_0\rho g_t^2 K_u}$ in the parentheses of Eq. (13), ζ in the vicinity of T_A and at $B_0 = 0$ becomes

$$\zeta \approx K\sqrt{\mu_0 M_l^2}\left[\frac{s^2}{K_u(a\delta_s^2 + K_u s^2)}\right]^{1/4}. \quad (14)$$

Two remarks are in order on the implications of Eq. (14). First, ζ in the vicinity of T_A is proportional to M_l, which is nonzero in ferrimagnets but zero in antiferromagnets. Therefore, ζ of antiferromagnets is proportional to $\sqrt{\mu_0\rho g_t^2 K_u}$ of Eq. (13), which is much smaller than $\sqrt{\mu_0 M_l^2}$ for ferrimagnets at T_A with sufficiently larger magnetization M_l. This suggests that ferrimagnets in the vicinity of T_A can show a much stronger magnon-photon coupling than antiferromagnets, because of the finite magnetization M_l.

Second, Eq. (14) shows that ζ for $B_0 = 0$ is the maximum at T_A where $\delta_s = 0$. Even for $B_0 \neq 0$, of which case can be directly computed from Eq. (12), ζ still exhibits the maximum in the vicinity of T_A [see Fig. 2(b)]. This enhanced ζ in the vicinity of T_A can be understood as follows. The denominator of Eq. (14) contains $a\delta_s^2$, which means that ζ is suppressed by the strong antiferromagnetic exchange interaction a as the net spin density δ_s increases: This is the reason why it exhibits the maximum at T_A with $\delta_s = 0$. This exchange-enhanced magnon-photon coupling in ferrimagnets becomes clearer by comparing two extreme cases. Exactly at T_A $(\delta_s = 0)$,

$$\zeta \approx K\sqrt{\mu_0 M_l^2}\left(\frac{1}{K_u}\right)^{1/2}. \quad (15)$$

Far away from T_A $(a\delta_s^2 \gg K_u s^2)$,

$$\zeta \approx K\sqrt{\mu_0 M_l^2}\left(\frac{1}{K_u a}\right)^{1/4}. \quad (16)$$

Comparing Eqs. (15) and (16), we find that ζ is exchange enhanced at T_A by the factor of $(a/K_u)^{1/4}$. It was suggested that this exchange-enhanced coupling

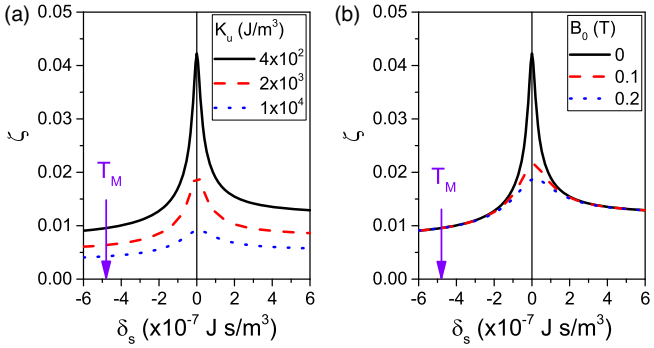

FIG. 2. The dimensionless effective magnon-photon coupling efficiency ζ of ferrimagnets as a function of the net spin density δ_s. Effects of (a) the uniaxial anisotropy K_u ($B_0 = 0$) and (b) the external field B_0 ($K_u = 4 \times 10^2$ J/m^3). We assume $M_1 = (1150 - 1.5x)$ kA/m and $M_2 = (1300 - 2.5x)$ kA/m, where a nominal variable x varies from 131 to 317. Other common parameters are $g_1 = 2.2$, $g_2 = 2.0$, and $A = 5 \times 10^{-12}$ J/m. T_M is the magnetic moment compensation point where $M_l = 0$.

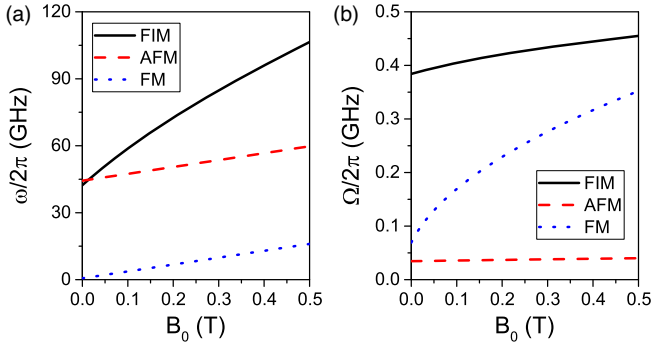

FIG. 3. Comparison of (a) the magnon frequency ω and (b) the magnon-photon coupling strength Ω as a function of the external field B_0 for ferrimagnet (FIM), antiferromagnet (AFM), and ferromagnet (FM). For FIM, $M_1 = 814$ kA/m, $M_2 = 740$ kA/m, $g_1 = 2.2$, and $g_2 = 2.0$ (i.e., $M_t = 1554$ kA/m, $M_l = 74$ kA/m, and $\delta_s = 0$). For AFM, $M_1 = M_2 = 777$ kA/m and $g_1 = g_2 = 2.2$ (i.e., $M_t = 1554$ kA/m and $M_l = 0$ kA/m). For FM, $M_1 = M_2 = 1000$ kA/m and $g_1 = g_2 = 2.2$ (i.e., $M_t = 2000$ kA/m). Common parameters are $K_u = 10^4$ J/m^3 and $A = 5 \times 10^{-12}$ J/m.

between antiferromagnetic magnons and other excitations is a general phenomenon originating from squeezing [46]. The exchange-enhanced magnon-magnon coupling was reported in ferrimagnets with a symmetry-breaking anisotropy that is essential to couple two magnon modes [45]. However, the exchange-enhanced magnon-photon coupling in ferrimagnets with the spin-rotational symmetry, as in this work, has not been reported.

Figure 2 shows ζ computed from Eq. (12) as a function of δ_s for various [Fig. 2(a)] K_u and [Fig. 2(b)] B_0. In all tested cases, ζ is the maximum in the vicinity of T_A, consistent with the above discussion. The maximum ζ decreases with increasing K_u or B_0, which originates from the fact that the magnon frequency (ω_+) increases more rapidly than the coupling strength Ω with increasing K_u or B_0. The magnetic moment compensation point T_M, where $M_l = 0$, is also indicated by an arrow. No special variation of ζ is observed at T_M, meaning that not the antiferromagnetic magnetization dynamics realized at T_M but the antiferromagnetic spin dynamics realized at T_A is important for the magnon-photon coupling.

Comparison with other types of magnets.—We compare the magnon frequency ω and the magnon-photon coupling strength Ω, instead of ζ, for ferromagnets, antiferromagnets, and ferrimagnets, because large values of both ω and Ω are beneficial for widespread application utilizing the magnon-photon coupling. We set $\delta_s = 0$ for FIM because the magnon-photon coupling in FIM is most efficient at T_A. We consider FM with uniaxial anisotropy and B_0 applied along the easy axis, as for FIM and AFM. With this anisotropy and field condition, we use the magnon-photon coupling model for FM in literature [17,27].

The magnon frequencies of three types of magnet are respectively given by $\omega_{\rm FM} = g_t(B_0 + B_K)$, $\omega_{\rm AFM} = \sqrt{K_u/\rho} + g_t B_0$, and $\omega_{\rm FIM} = \sqrt{(K_u + M_l B_0)/\rho} + g_t B_0$, where $B_K = 4K_u/M_t$ is the uniaxial anisotropy field. It is well known that $\omega_{\rm AFM} \gg \omega_{\rm FM}$ because of the antiferromagnetic exchange in AFM [35–37]. Except for a finite Zeeman coupling (i.e., $M_l B_0$) in $\omega_{\rm FIM}$, the magnon frequencies of AFM and FIM are of the same form. Therefore, the condition of $\omega_{\rm AFM} \approx \omega_{\rm FIM} \gg \omega_{\rm FM}$ holds in general even though a precise comparison depends on material parameters.

On the other hand, the magnon-photon coupling strengths of FM, AFM, and FIM are respectively given by

$$\Omega_{\rm FM} = K g_t \sqrt{\mu_0 M_t (B_0 + B_K)},$$
$$\Omega_{\rm AFM} = K \sqrt{\mu_0 g_t^2 (K_u + B_0 g_t \sqrt{\rho K_u})},$$
$$\Omega_{\rm FIM} = K \left(1 + \frac{M_l}{g_t X}\right) \sqrt{\mu_0 g_t^2 [K_u + B_0 (M_l + g_t X)]}, \quad (17)$$

where $X = \sqrt{\rho(K_u + M_l B_0)}$ is a certain quantity in unit of spin density. When $B_0 = 0$, $\Omega_{\rm AFM} = K\sqrt{\mu_0 g_t^2 K_u}$ and $\Omega_{\rm FIM} = K(\sqrt{\mu_0 M_l^2} + \sqrt{\mu_0 \rho g_t^2 K_u})/\sqrt{\rho}$. Given $\sqrt{\mu_0 M_l^2} \gg \sqrt{\mu_0 \rho g_t^2 K_u}$ [see the above discussion for ζ below Eq. (13)], the ratio $\Omega_{\rm FIM}/\Omega_{\rm AFM} \approx \sqrt{M_l^2/\rho g_t^2 K_u}$ is much larger than 1, provided that M_l at T_A is sufficiently large. This result shows that a finite net magnetic moment M_l at T_A of FIM can greatly enhance the magnon-photon coupling in comparison to AFM.

Figure 3(a) shows ω and Fig. 3(b) shows Ω as a function of B_0 for FIM, AFM, and FM with reasonable parameters listed in the caption. We find $\omega_{\rm FIM} \approx \omega_{\rm AFM} \gg \omega_{\rm FM}$ and $\Omega_{\rm FIM} > \Omega_{\rm FM} > \Omega_{\rm AFM}$. These orders of ω and Ω for the three types of magnet are found to be maintained with some variations of parameters. For instance, the orders of ω and

Ω are maintained even with 10 times increase of K_u (not shown). This result shows that FIM not only simply combines the best features of AFM (i.e., high ω) and FM (i.e., high Ω), but also enables the largest Ω among different types of magnet.

Discussion.—In this Letter, we investigate the magnon-photon coupling in an antiferromagnetically coupled ferrimagnet consisting of two inequivalent magnetic atoms with different Landé-g factors. We show that the effective magnon-photon coupling ζ is exchange enhanced at T_A. Moreover, both relevant magnon frequency ω and magnon-photon coupling strength Ω can be large for ferrimagnets at T_A. This result will be useful to expand the research scope and application area of magnon-photon coupling. For instance, RE-TM ferrimagnets are most often employed for all-optical magnetization switching [49–51], which would also be related to the magnon-photon coupling, but the role of net spin density in all-optical magnetization switching has remained unexplored.

We finally suggest possible candidates of ferrimagnets for the experimental test of our prediction. Two important conditions for the material choice are (1) a clear difference between T_M and T_A and (2) sufficiently low damping. These conditions are met by GdFeCo with $|T_M - T_A| \approx 90$ K [38] and a low damping of $(3.2\text{–}7.2) \times 10^{-3}$ [52,53]. At T_A, $\omega/2\pi$ and $\Omega/2\pi$ of GdFeCo are respectively estimated to be 68 GHz and 322 MHz with the following parameters: $M_l = 3.9 \times 10^4$ A/m [53], $K_u = 3.8 \times 10^4$ J/m^3 [54], $J = 2.1 \times 10^{-22}$ J [55], $K = 0.016$ [17], $B_0 = 0.3$ T [17], and $d = 0.4$ nm. The estimated ω and Ω are larger than those of YIG [17]. Single crystalline RE-doped garnets are also possible candidates. Among them, gadolinium iron garnet (GdIG) has a low damping [56], but an early experiment reported that T_A and T_M would be close to each other [57], demanding a further experimental investigation for GdIG. Alternatively, mixed substituted RE-doped iron garnets $R_xGd_{3-x}Fe_5O_{12}$ (R = Tb, Dy, Ho, Er, Tm, and Yb) could be considered because the $4f$ shell of the above-listed rare-earth elements (R) is not half-filled. One concern is that substituting Gd by R may increase the damping [56]. In this respect, it is valuable to experimentally investigate T_A, T_M, and damping of $R_xGd_{3-x}Fe_5O_{12}$ as a function of R and its composition.

The authors acknowledge T. Ono and C. A. Ross for fruitful discussion. K.-J. L. was supported by the National Research Foundation (NRF) of Korea (NRF-2020R1A2C3013302). S. K. K. was supported by the startup fund at the University of Missouri.

*sekwonkim@kaist.ac.kr
†kj_lee@korea.ac.kr

[1] M. A. Nielsen and I. L. Chuang, *Quantum Computation and Quantum Information* (Cambridge University Press, Cambridge, England, 2000).
[2] R. Blatt and D. Wineland, Nature (London) **453**, 1008 (2008).
[3] Y. Makhlin, G. Schön, and A. Shnirman, Rev. Mod. Phys. **73**, 357 (2001).
[4] J. Wrachtrup and F. Jelezko, J. Phys. Condens. Matter **18**, S807 (2006).
[5] I. Buluta, S. Ashhab, and F. Nori, Rep. Prog. Phys. **74**, 104401 (2011).
[6] Z. L. Xiang, S. Ashhab, J. Q. You, and F. Nori, Rev. Mod. Phys. **85**, 623 (2013).
[7] G. Kurizki, P. Bertet, Y. Kubo, K. Mølmer, D. Petrosyan, P. Rabl, and J. Schmiedmayer, Proc. Natl. Acad. Sci. U.S.A. **112**, 3866 (2015).
[8] A. Imamoğlu, Phys. Rev. Lett. **102**, 083602 (2009).
[9] J. H. Wesenberg, A. Ardavan, G. A. D. Briggs, J. J. L. Morton, R. J. Schoelkopf, D. I. Schuster, and K. Mølmer, Phys. Rev. Lett. **103**, 070502 (2009).
[10] M. G. Raizen, R. J. Thompson, R. J. Brecha, H. J. Kimble, and H. J. Carmichael, Phys. Rev. Lett. **63**, 240 (1989).
[11] Ö. O. Soykal and M. E. Flatté, Phys. Rev. Lett. **104**, 077202 (2010).
[12] H. Huebl, C. W. Zollitsch, J. Lotze, F. Hocke, M. Greifenstein, A. Marx, R. Gross, and S. T. B. Goennenwein, Phys. Rev. Lett. **111**, 127003 (2013).
[13] X. Zhang, C.-L. Zou, L. Jiang, and H. X. Tang, Phys. Rev. Lett. **113**, 156401 (2014).
[14] Y. Tabuchi, S. Ishino, T. Ishikawa, R. Yamazaki, K. Usami, and Y. Nakamura, Phys. Rev. Lett. **113**, 083603 (2014).
[15] M. Goryachev, W. G. Farr, D. L. Creedon, Y. Fan, M. Kostylev, and M. E. Tobar, Phys. Rev. Applied **2**, 054002 (2014).
[16] Y. Cao, P. Yan, H. Huebl, S. T. B. Goennenwein, and G. E. W. Bauer, Phys. Rev. B **91**, 094423 (2015).
[17] L. Bai, M. Harder, Y. P. Chen, X. Fan, J. Q. Xiao, and C.-M. Hu, Phys. Rev. Lett. **114**, 227201 (2015).
[18] J. A. Haigh, S. Langenfeld, N. J. Lambert, J. J. Baumberg, A. J. Ramsay, A. Nunnenkamp, and A. J. Ferguson, Phys. Rev. A **92**, 063845 (2015).
[19] H. Maier-Flaig, M. Harder, R. Gross, H. Huebl, and S. T. B. Goennenwein, Phys. Rev. B **94**, 054433 (2016).
[20] A. Osada, R. Hisatomi, A. Noguchi, Y. Tabuchi, R. Yamazaki, K. Usami, M. Sadgrove, R. Yalla, M. Nomura, and Y. Nakamura, Phys. Rev. Lett. **116**, 223601 (2016).
[21] X. Zhang, N. Zhu, C.-L. Zou, and H. X. Tang, Phys. Rev. Lett. **117**, 123605 (2016).
[22] D. Lachance-Quirion, Y. Tabuchi, S. Ishino, A. Noguchi, T. Ishikawa, R. Yamazaki, and Y. Nakamura, Sci. Adv. **3**, e1603150 (2017).
[23] B. M. Yao, Y. S. Gui, J. W. Rao, S. Kaur, X. S. Chen, W. Lu, Y. Xiao, H. Guo, K.-P. Marzlin, and C.-M. Hu, Nat. Commun. **8**, 1437 (2017).
[24] L. Bai, M. Harder, P. Hyde, Z. Zhang, C.-M. Hu, Y. P. Chen, and J. Q. Xiao, Phys. Rev. Lett. **118**, 217201 (2017).
[25] Y.-P. Wang, G.-Q. Zhang, D. Zhang, T.-F. Li, C.-M. Hu, and J. Q. You, Phys. Rev. Lett. **120**, 057202 (2018).
[26] M. Harder, Y. Yang, B. M. Yao, C. H. Yu, J. W. Rao, Y. S. Gui, R. L. Stamps, and C.-M. Hu, Phys. Rev. Lett. **121**, 137203 (2018).
[27] V. L. Grigoryan, K. Shen, and K. Xia, Phys. Rev. B **98**, 024406 (2018).

[28] B. Bhoi, B. Kim, S.-H. Jang, J. Kim, J. Yang, Y.-J. Cho, and S.-K. Kim, Phys. Rev. B **99**, 134426 (2019).
[29] Y. Li, T. Polakovic, Y.-L. Wang, J. Xu, S. Lendinez, Z. Zhang, J. Ding, T. Khaire, H. Saglam, R. Divan, J. Pearson, W.-K. Kwok, Z. Xiao, V. Novosad, A. Hoffmann, and Wei Zhang, Phys. Rev. Lett. **123**, 107701 (2019).
[30] J. T. Hou and L. Liu, Phys. Rev. Lett. **123**, 107702 (2019).
[31] W. Yu, J. Wang, H. Y. Yuan, and J. Xiao, Phys. Rev. Lett. **123**, 227201 (2019).
[32] H. Y. Yuan and X. R. Wang, Appl. Phys. Lett. **110**, 082403 (2017).
[33] M. Mergenthaler, J. Liu, J. J. Le Roy, N. Ares, A. L. Thompson, L. Bogani, F. Luis, S. J. Blundell, T. Lancaster, A. Ardavan, G. A. D. Briggs, P. J. Leek, and E. A. Laird, Phys. Rev. Lett. **119**, 147701 (2017).
[34] Ø. Johansen and A. Brataas, Phys. Rev. Lett. **121**, 087204 (2018).
[35] F. Keffer and C. Kittel, Phys. Rev. **85**, 329 (1952).
[36] T. Kampfrath, A. Sell, G. Klatt, A. Pashkin, S. Mährlein, T. Dekorsy, M. Wolf, M. Fiebig, A. Leitenstorfer, and R. Huber, Nat. Photonics **5**, 31 (2011).
[37] T. Jungwirth, X. Marti, P. Wadley, and J. Wunderlich, Nat. Nanotechnol. **11**, 231 (2016).
[38] K.-J. Kim, S. K. Kim, Y. Hirata, S.-H. Oh, T. Tono, D.-H. Kim, T. Okuno, W. S. Ham, S. Kim, G. Go, Y. Tserkovnyak, A. Tsukamoto, T. Moriyama, K.-J. Lee, and T. Ono, Nat. Mater. **16**, 1187 (2017).
[39] S.-H. Oh, S. K. Kim, D.-K. Lee, G. Go, K.-J. Kim, T. Ono, Y. Tserkovnyak, and K.-J. Lee, Phys. Rev. B **96**, 100407(R) (2017).
[40] L. Caretta, M. Mann, F. Büttner, K. Ueda, B. Pfau, C. M. Günther, P. Hessing, A. Churikova, C. Klose, M. Schneider, D. Engel, C. Marcus, D. Bono, K. Bagschik, S. Eisebitt, and G. S. D. Beach, Nat. Nanotechnol. **13**, 1154 (2018).
[41] S. A. Siddiqui, J. Han, J. T. Finley, C. A. Ross, and L. Liu, Phys. Rev. Lett. **121**, 057701 (2018).
[42] S.-H. Oh and K.-J. Lee, J. Magn. **23**, 196 (2018).
[43] S. K. Kim, K.-J. Lee, and Y. Tserkovnyak, Phys. Rev. B **95**, 140404(R) (2017).
[44] Y. Hirata, D.-H. Kim, S. K. Kim, D.-K. Lee, S.-H. Oh, D.-Y. Kim, T. Nishimura, T. Okuno, Y. Futakawa, H. Yoshikawa, A. Tsukamoto, Y. Tserkovnyak, Y. Shiota, T. Moriyama, S.-B. Choe, K.-J. Lee, and T. Ono, Nat. Nanotechnol. **14**, 232 (2019).
[45] L. Liensberger, A. Kamra, H. Maier-Flaig, S. Geprägs, A. Erb, S. T. B. Goennenwein, R. Gross, W. Belzig, H. Huebl, and M. Weiler, Phys. Rev. Lett. **123**, 117204 (2019).
[46] A. Kamra, E. Thingstad, G. Rastelli, R. A. Duine, A. Brataas, W. Belzig, and A. Sudbø, Phys. Rev. B **100**, 174407 (2019).
[47] E. G. Tveten, A. Qaiumzadeh, and A. Brataas, Phys. Rev. Lett. **112**, 147204 (2014).
[48] K. M. D. Hals, Y. Tserkovnyak, and A. Brataas, Phys. Rev. Lett. **106**, 107206 (2011).
[49] C. D. Stanciu, F. Hansteen, A. V. Kimel, A. Kirilyuk, A. Tsukamoto, A. Itoh, and Th. Rasing, Phys. Rev. Lett. **99**, 047601 (2007).
[50] I. Radu, K. Vahaplar, C. Stamm, T. Kachel, N. Pontius, H. A. Dürr, T. A. Ostler, J. Barker, R. F. L. Evans, R. W. Chantrell, A. Tsukamoto, A. Itoh, A. Kirilyuk, Th. Rasing, and A. V. Kimel, Nature (London) **472**, 205 (2011).
[51] S. Mangin, M. Gottwald, C-H. Lambert, D. Steil, V. Uhlíř, L. Pang, M. Hehn, S. Alebrand, M. Cinchetti, G. Malinowski, Y. Fainman, M. Aeschlimann, and E. E. Fullerton, Nat. Mater. **13**, 286 (2014).
[52] D.-H. Kim, T. Okuno, S. K. Kim, S.-H. Oh, T. Nishimura, Y. Hirata, Y. Futakawa, H. Yoshikawa, A. Tsukamoto, Y. Tserkovnyak, Y. Shiota, T. Moriyama, K.-J. Kim, K.-J. Lee, and T. Ono, Phys. Rev. Lett. **122**, 127203 (2019).
[53] T. Okuno, D.-H. Kim, S.-H. Oh, S. K. Kim, Y. Hirata, T. Nishimura, W. S. Ham, Y. Futakawa, H. Yoshikawa, A. Tsukamoto, Y. Tserkovnyak, Y. Shiota, T. Moriyama, K.-J. Kim, K.-J. Lee, and T. Ono, National electronics review **2**, 389 (2019).
[54] M. Ding and S. J. Poon, J. Magn. Magn. Mater. **339**, 51 (2013).
[55] P. Hansen, C. Clausen, G. Much, M. Rosenkranz, and K. Witter, J. Appl. Phys. **66**, 756 (1989).
[56] G. P. Vella-Coleiro, D. H. Smith, and L. G. Van Uitert, Appl. Phys. Lett. **21**, 36 (1972).
[57] B. A. Calhoun, J. Overmeyer, and W. V. Smith, Phys. Rev. **107**, 993 (1957).